

1 **Supplementary Information**

2

3 **Gold nanorods-paper electrode based enzyme-free electrochemical immunoassay of prostate**  
4 **specific antigen using porous zinc oxide spheres-silver nanoparticles nanocomposites as**  
5 **labels**

6 Guoqiang Sun,<sup>a</sup> Haiyun Liu,<sup>a</sup> Yan Zhang,<sup>a</sup> Jinghua Yu,<sup>a</sup> Mei Yan,<sup>\*a</sup> Xianrang Song<sup>b</sup> and

7 Wenxing He<sup>\*c</sup>

8

9 *<sup>a</sup>Key Laboratory of Chemical Sensing & Analysis in Universities of Shandong, School of*  
10 *Chemistry and Chemical Engineering, University of Jinan, Jinan 250022, China*

11 *<sup>b</sup>Cancer Research Center Shandong Tumor Hospital, Jinan 250117, China*

12 *<sup>c</sup>School of Biological Sciences and Technology, University of Jinan, Jinan 250022, China*

13

14 \*Corresponding authors: Mei Yan; Wenxing He

15 E-mail: [chm526yanm@gmail.com](mailto:chm526yanm@gmail.com); 163.x@163.com

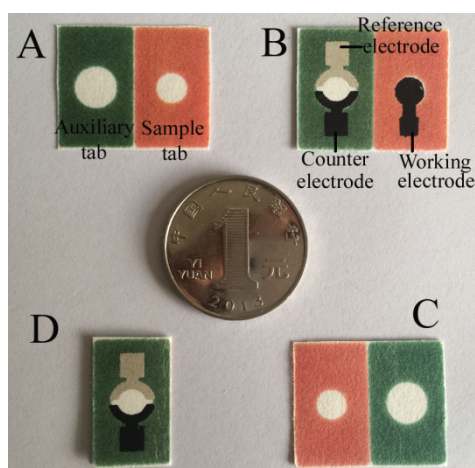
16 Telephone: +86-531-82767161

17

## 18 Preparation of the electrochemical origami device

19 Wax-screen-printing was used to build the origami EC device. The fabrication process consisted  
20 of wax-printing, baking the wax-patterned sheet, followed by screen-printing electrodes. Firstly,  
21 The shape of the hydrophobic barrier on the origami device, which contained a paper auxiliary  
22 zone (8 mm in diameter) on the auxiliary tab (12.0 mm × 20.0 mm), and a paper sample zone (6.0  
23 mm in diameter) on the sample tab (12.0 mm × 20.0 mm), respectively (Scheme S1A), was  
24 designed using Adobe illustrator CS4. Then, the entire origami device could be produced in bulk  
25 on an A4 paper sheet using a commercially available solid-wax printer (Xerox Phaser 8560N color  
26 printer). Owing to the porous structure of paper, the melted wax could penetrate into the paper  
27 network to decrease the hydrophilicity of paper remarkably. Meanwhile, the unprinted area (paper  
28 auxiliary zone and paper sample zone) still maintained good hydrophilicity, flexibility, and porous  
29 structure and will not affect the further screen-printing of electrodes and modifications.

30 The electrode arrays consisted of a screen-printed Ag/AgCl reference electrode and carbon  
31 counter electrode on the paper auxiliary zone and a screen-printed carbon working electrode on  
32 the paper sample zone (Scheme S1B and S1C). Between the sample tab and auxiliary tab, the  
33 unprinted line (1 mm in width) was defined as the fold line, which could ensure that the paper  
34 sample zone on the sample tab was properly and exactly aligned to the auxiliary zone on the  
35 auxiliary tab after folding (Scheme S1D), due to the difference of flexibility between the printed  
36 and unprinted area after baking. After folding, the three screen-printed electrodes (working  
37 electrode, reference electrode, and counter electrode) will be connected once the paper EC cell has  
38 been filled with solution.



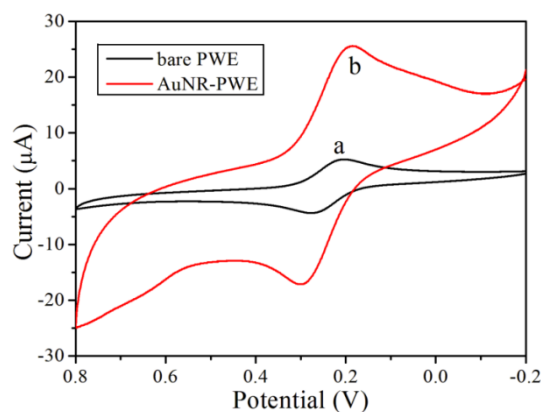
39

40 **Scheme S1.** The photo images of (A) the origami device, (B) One side of the device with the

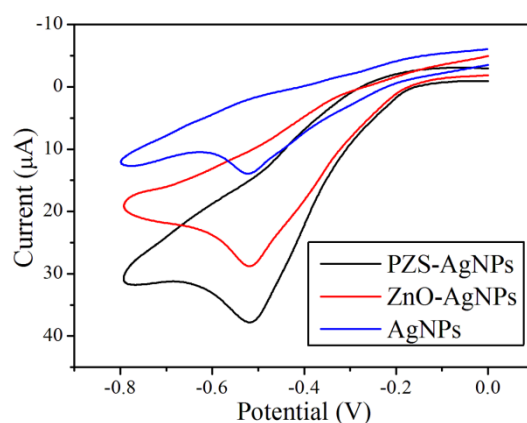
41 screen-printed working, reference and counter electrode, (C) the other side of the device and (D)  
42 the origami device after folding down the sample tab below the auxiliary tab.  
43

#### 44 Preparation of PZS-AgNPs-Ab<sub>2</sub>

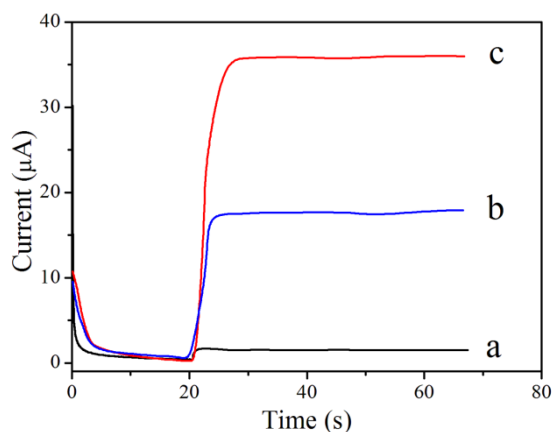
45 The preparation procedure of the PZS-AgNPs-Ab<sub>2</sub> bioconjugate was as follows: 1.0 mg of the as-  
46 prepared PZS-AgNPs was dispersed into 1.0 mL of pH 7.4 PBS. Followed by ultrasonication for 5  
47 min, 10  $\mu\text{L}$  of Ab<sub>2</sub> (20  $\mu\text{g mL}^{-1}$ ) was added into the solution, and then the mixture was slightly  
48 vortexed for 4 h. Subsequently, free antibodies were removed by centrifugation and washing with  
49 PBS (pH 7.4) for several times to obtain the Ab<sub>2</sub> modified PZS-AgNPs. Next, the precipitate of  
50 PZS-AgNPs antibodies conjugates was dispersed with 1.0 mL of 1% BSA solution to block the  
51 nonspecific binding sites. Finally, the resultant PZS-AgNPs-Ab<sub>2</sub> were dispersed with PBS (pH 7.4)  
52 to a final volume of 1.0 mL and stored at 4 °C for later use.



53  
54 **Fig. S1.** CVs of (a) bare PWE and (b) AuNRs-PWE in 5.0 mM  $[\text{Fe}(\text{CN})_6]^{3-/4-}$  solution containing  
55 0.5 M KCl.



56  
57 **Fig. S2.** CVs of the different immunosensors constructed with various signal label using 1.0 ng  
58  $\text{mL}^{-1}$  PSA as model.



59

60 **Fig. S3.** Current responses of the immunosensor with different concentration of PSA: (a) 0 ng mL<sup>-1</sup>,  
 61 (b) 0.05 ng mL<sup>-1</sup>, (c) 1.0 ng mL<sup>-1</sup>.

62

### 63 **Optimization of assay conditions**

64 To achieve an optimal electrochemical signal, the experimental conditions were optimized. During  
 65 the immunosensor preparation process, the same concentration of PSA (1.0 ng mL<sup>-1</sup>) was used to  
 66 fabricate the immunosensor. The temperature of the antigen-antibody reaction greatly affected the  
 67 sensitivity of the immunosensor. In general, 37 °C, close to the normal temperature of the human  
 68 body, was favorable for the antigen-antibody interaction. Considering the practical application  
 69 hereafter, all the experiments were carried out at room temperature.

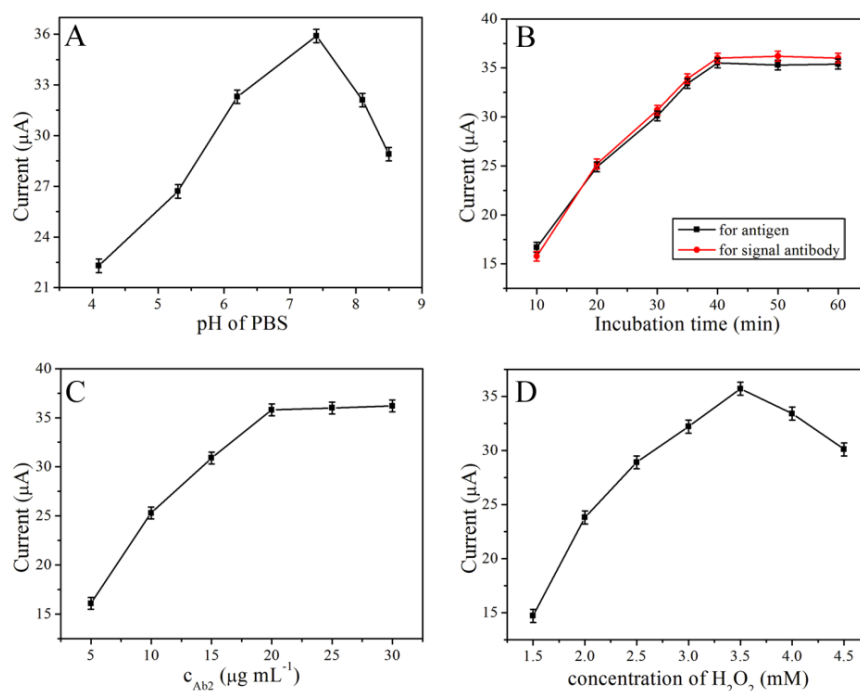
70 As we know, highly acidic or alkaline surroundings would damage the immobilized protein,  
 71 especially in alkalinity. Fig. S4A showed the effects of pH on the current responses of the  
 72 immunosensor. The currents increased steeply with the increase of pH from 4.1 to 7.4, and then  
 73 decreased from 7.4 to 8.5. An optimal amperometric response was achieved at pH 7.4. Hence, pH  
 74 7.4 of PBS was selected as the electrolyte for PSA detection.

75 The incubation time was also an important parameter for both capture PSA and signal  
 76 antibody on the electrode surface. As seen from Fig. S4B, the electrochemical response increased  
 77 with increasing incubation time of PSA antigen, and then tended to a steady value after 40 min,  
 78 indicating a thorough capturing of the antigens on the electrode surface. In the second  
 79 immunoassay incubation step, the current showed the same changing tendency, and the response  
 80 current reached a plateau at about 40 min. Longer incubation time did not improve the response.  
 81 Therefore, 40 min was selected as the incubation time for determination of PSA in this study.

82 Because of the immobilization of antibodies on the PZS-AgNPs nanocarrier, the ratio of

83 antibodies and nanocarrier was an important factor on the response signal. To define the ratio of  
 84 Ab<sub>2</sub> and PZS-AgNPs, we use different concentration of Ab<sub>2</sub> to label the carrier. It could be seen  
 85 that with the augment of Ab<sub>2</sub> concentration at lower concentration, the signal intensity increased  
 86 dramatically. Then the trend gradually slowed down till the Ab<sub>2</sub> concentration up to 20 μg mL<sup>-1</sup>  
 87 indicating the occurrence of the saturation concentration (Fig. S4C). Accordingly, 20 μg·mL<sup>-1</sup> Ab<sub>2</sub>  
 88 was used to label the nanocarrier.

89 To adequately release the catalytic efficiency of carrier PZS-AgNPs, the concentration of the  
 90 added H<sub>2</sub>O<sub>2</sub> in PBS (pH 7.4) should be optimized. Higher concentration of H<sub>2</sub>O<sub>2</sub> might inhibit the  
 91 catalysis, while the catalysis could not be completely embodied at lower concentration. As shown  
 92 in Fig. S4D, one can see that catalytic current increased with increasing the concentration of H<sub>2</sub>O<sub>2</sub>,  
 93 and the maximum response was achieved at 3.5 mM H<sub>2</sub>O<sub>2</sub>. Therefore, 3.5 mM H<sub>2</sub>O<sub>2</sub> was selected  
 94 as the optimal condition to detect PSA.

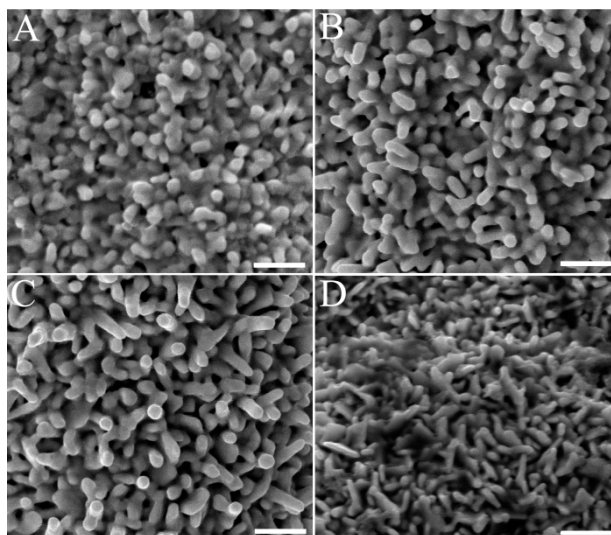


95  
 96 **Fig. S4.** Influence of (A) pH of PBS, (B) incubation time, concentration of (C) Ab<sub>2</sub> and (D) H<sub>2</sub>O<sub>2</sub>  
 97 on current response of the immunosensor. The data was recorded in PBS solution (pH 7.4)  
 98 containing 3.5 mM H<sub>2</sub>O<sub>2</sub> at -0.52 V. n = 11 for each point, error bars represent standard deviation  
 99 standard deviation (SD).

100

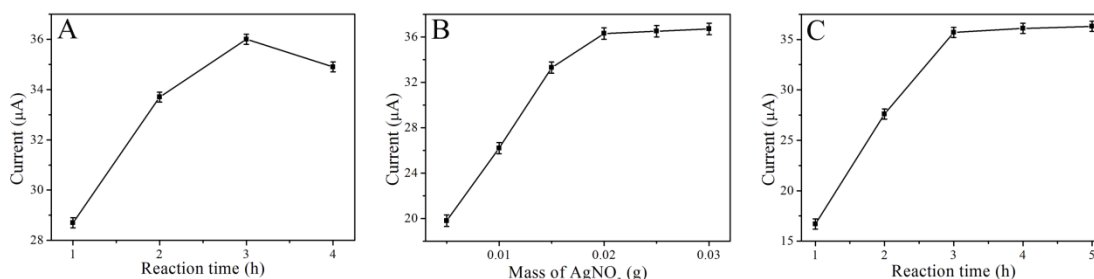
101 The AuNRs modified paper electrode was fabricated at 95 °C for 3 h. With the increase of  
 102 reaction time, the amount of AuNRs on paper electrode increased and the morphology of AuNRs  
 103 became uniform. However, the longer reaction time changed the structure of AuNRs (Fig. S5).

104 Meanwhile, these paper electrodes were used to construct immunosensors under same condition  
105 using  $1.0 \text{ ng mL}^{-1}$  PSA, respectively. As shown in Fig. S6A, the current response increased with  
106 the increasing of reaction time, and the maximum response was achieved at reaction time 3 h. This  
107 may attributed to the AuNRs obtained at 3 h owned largest surface area and electronic  
108 transmission rate. Thus, 3 h was chosen as optimal reaction time to synthesize AuNRs modified  
109 paper electrode.



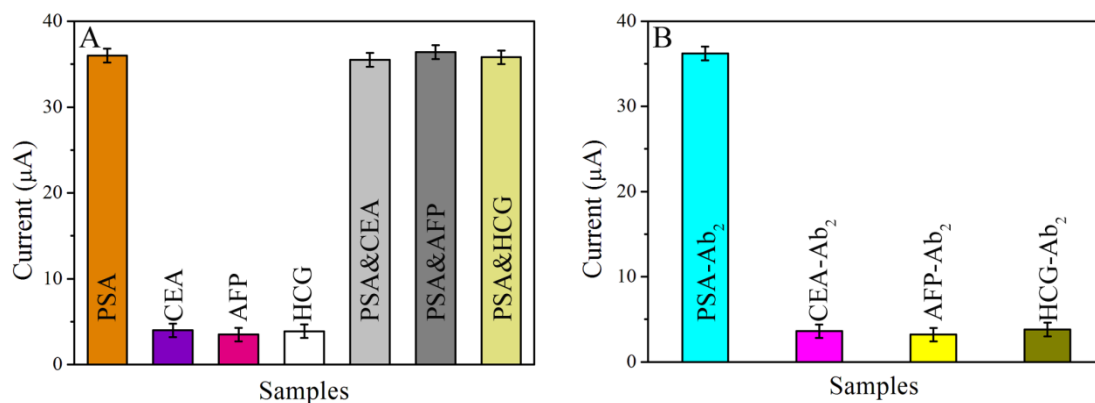
110  
111 **Fig. S5.** SEM images of AuNRs modified paper electrode with different reaction: (A) 1 h, (B) 2 h,  
112 (C) 3 h, (D) 4 h. Scale bar = 500 nm.

113  
114 AgNPs owned high catalytic activity toward  $\text{H}_2\text{O}_2$  reduction. The content of AgNPs in PZS-  
115 AgNPs composites was adjusted by the addition mass of  $\text{AgNO}_3$  and reaction time. As shown in  
116 Fig. S6B, the current response increased with the increasing of addition mass of  $\text{AgNO}_3$  and then  
117 leveled off at 0.02 g of  $\text{AgNO}_3$ , which indicated a saturated loading AgNPs on PZS. Meanwhile,  
118 the current response showed the same changing tendency, and the current reached a plateau at  
119 reaction time of 3 h (Fig. S6C). Therefore, 0.02 g of  $\text{AgNO}_3$  and reaction time of 3 h were selected  
120 to fabricate PZS-AgNPs composites.



121  
122 **Fig. S6.** Influence of (A) reaction time in fabrication of AuNRs-PWE, (B) additional mass of  
123  $\text{AgNO}_3$  in fabrication of PZS-AgNPs, (C) reaction time in fabrication of PZS-AgNPs on current

124 response of the immunosensor. n = 11 for each point, error bars represent standard deviation SD.  
 125



126  
 127 **Fig. S7.** The interfering effects of (A) sample matrix components and (B) signal antibodies on the  
 128 current responses of the electrochemical immunosensor. n = 11 for each bar, error bars represent  
 129 SD.

130

131 **Table S1.** Comparison of analytical properties of different immunoassays toward PSA

Electrode	Signal label	Linear range (ng mL <sup>-1</sup> )	Detection limit (ng mL <sup>-1</sup> )	References
MPS/ITO	SiO <sub>2</sub> @C-dots	0.01-50	0.003	1
GE-CHIT/GCE	GOx-GNR	0.01-8	0.008	2
Au electrode	ferrocene-helix peptide	0.5-40	0.2	3
Au electrode	G-quadruplex-hemin DNAzyme	0.14-1400	0.14	4
AuNR-PWE	PZS-AgNPs	0.004-60	0.0015	This work

132 **References**

- 133 1 Y. Zhang, W. Y. Liu, S. G. Ge, M. Yan, S. W. Wang, J. H. Yu, N. Q. Li and X. R. Song,  
 134 *Biosens. Bioelectron.*, 2013, **41**, 684-690.  
 135 2 S. J. Xu, Y. Liu, T. H. Wang and J. H. Li, *Anal. Chem.*, 2011, **83**, 3817-3823.  
 136 3 N. Zhao, Y. Q. He, X. Mao, Y. H. Sun, X. B. Zhang, C. Z. Li, Y. H. Lin and G. D. Liu,  
 137 *Electrochem. Commun.*, 2010, **12**, 471-474.  
 138 4 J. Liu, C. Y. Lu, H. Zhou, J. J. Xu, Z. H. Wang and H. Y. Chen, *Chem. Commun.*, 2013, **49**,  
 139 6602-6604.